EEET ECOLOGICAL ENGINEERING & ENVIRONMENTAL TECHNOLOGY

Ecological Engineering & Environmental Technology, 2026, 27(8), 322–344
https://doi.org/10.12912/27197050/225391
ISSN 2719–7050, License CC-BY 4.0

Received: 2026.06.25
Accepted: 2026.07.10
Published: 2026.08.01

Improving soil erodibility estimation using a plasticity-based K factor in a Mediterranean basin: A case study from Northern Morocco

Imad Ghadouani[1*], Nadia Machouri[1]

[1] Department of Geography, Faculty of Letters and Human Sciences, Mohammed V University, Rabat, Morocco
* Corresponding author's e-mail: imad_ghadouani@um5.ac.ma

ABSTRACT

Soil erodibility is a critical parameter in erosion modeling, yet conventional RUSLE K-factors often overestimate soil loss due to the lack of local calibration, particularly in Mediterranean regions. This study develops a locally calibrated K-factor for the Oued Aoudour basin (Moroccan Rif) based on the plasticity index (PI) and lithological controls, with qualitative field support from a custom-built rainfall simulator. A logarithmic regression between K_observed and ln (PI) was established using 11 samples representing the main lithological units. After integrating a lithological factor (F_lith_capped) and a final empirical correction factor (0.603587229), the model performance improved from $R^2 = 0.465$ to $R^2 = 0.9918$. Leave-one-out cross-validation confirmed internal stability ($R^2 = 0.985$). The developed K-factor ranged from 0.0332 (calcareous soils) to 0.2662 (flysch soils), with estimated soil loss averaging 39 t/ha/year – a 32% improvement over the conventional K-factor (52 t/ha/year). Field measurements using the rainfall simulator (10–12 t/ha/year) provided qualitative support for the model's improved relative performance. The proposed PI-based K-factor offers a simple, low-cost, and transferable approach for improving RUSLE-based erosion assessments in Mediterranean basins and data-scarce regions worldwide.

Keywords: soil erosion, RUSLE, soil erodibility factor, plasticity index, rainfall simulation, Éric Roose methodology, Mediterranean basin, Morocco.

INTRODUCTION

Water erosion is considered one of the major environmental issues threatening ecosystems, reducing agricultural productivity, and causing annual soil quality degradation (Issaka and Ashraf, 2017; Sonderegger and Pfister, 2021). According to data from the Food and Agriculture Organization (FAO, 2015), approximately 33% of the world's soils are currently degraded, and this proportion may exceed 90% by 2050. In Morocco, numerous studies have addressed the estimation and spatial analysis of water erosion (El Assaoui et al., 2023; Laouina, 2010; Moussebbih et al., 2019; Sadiki et al., 2004). Erosion mapping is considered an essential step for identifying the spatial variability of soil loss rates, detecting the most vulnerable areas, and assessing erosion severity in support of natural resource management.

Erosion rates in Morocco exhibit significant spatial variability. In some cases, values exceed 50 t/ha/year (Administration des Eaux et Forêts et de la Conservation des Sols, 1995; Amhani and Tribak, 2022; Brahim et al., 2020; Dahman et al., 1997; Ed-Dakiri et al., 2024; Ghadouani and Machouri, 2026; Najem et al., 2026), whereas annual averages in other regions, such as the Middle Atlas and High Atlas, do not exceed 20 t/ha/year. This variability reflects the influence of complex interactions among climatic, geological, and topographic characteristics.

Soil loss can be estimated using two principal approaches: direct (field-based) and indirect (model-based) methods. The direct methods adopted in this study are highly accurate despite requiring substantial field effort, long monitoring periods, and high operational costs (Duarte and Teodoro, 2021). In contrast, indirect methods rely on predictive mathematical models, which have experienced remarkable development owing to advances in geographic information systems (GIS) and remote sensing (RS) technologies, making them increasingly applied in large-scale environmental studies.

Among these models, the Rusle model is one of the most widely used tools for estimating water erosion (Renard et al, 1997). The model incorporates five main factors: rainfall erosivity factor (R), soil erodibility factor (K), topographic factor (LS), cover-management factor (C), and conservation practice factor (P). Among these parameters, the soil erodibility factor (K) is considered one of the most critical and sensitive components due to its role in expressing the intrinsic properties of soils and their resistance to detachment and transport processes.

Traditional methods for estimating the K factor are based on empirical equations developed by (Wischmeier and Smith, 1978) in environmental conditions different from those of the Mediterranean region (Nzereogu et al., 2023; Rehman et al., 2025). Consequently, these equations may not accurately reflect local geological specificities, particularly in complex environments such as northern Morocco. Despite the extensive application of the RUSLE model, estimating the K factor remains a major challenge in Mediterranean areas, especially within the Aoudour Basin (Central Rif), where strong lithological diversity, including marls, flysch formations, and carbonate rocks, generates soils with highly variable physical and geotechnical properties.

Preliminary investigations demonstrated that applying the conventional (Wischmeier and Smith, 1978) factor in this region produced an average soil loss estimate of 52 t/ha/year, which was significantly higher than the initial field measurements. This discrepancy highlights the necessity of developing a local factor capable of accounting for the specific characteristics of regional soils.

In this context, integrating geotechnical indicators, particularly the Plasticity index (PI), has become increasingly important for estimating soil erodibility. Derived from the Atterberg Limits, the PI reflects soil cohesion and resistance to disintegration, making it directly related to detachment and transport processes. However, the relationship between the plasticity index and soil erodibility has not been sufficiently investigated in the Moroccan context.

To date, no study has successfully integrated the PI with lithological factors to calibrate the RUSLE K-factor in the Mediterranean basin. Furthermore, previous works have treated the relationship between PI and K as linear, resulting in low predictive power ($R^2 < 0.7$). This study establishes, for the first time, a logarithmic relationship between PI and K, achieving an exceptional $R^2 = 0.9918$ after integrating lithological and correction factors.

This study was based on 11 soil samples (S1 to S11) representing the main lithological units of the Oued Aoudour Basin, including Quaternary cover (Q), Triassic formations (Tr), Mio-marl formations (Mio-Mar), Numidian units (Num), flysch formations (Fly), Upper M.C. flysch (Fly-MCsup), Middle M.C. flysch (Fly-Cmoy), dolomitic limestone (Cal-Dol), and Jurassic limestone (Cal-Jur). The measured PI values ranged from 0.69 for calcareous soils to 35 for Quaternary deposits, while K_observed values varied between 0.05 and 0.39.

The novelty of this study lies in three interconnected contributions: (1) to our knowledge, this is the first logarithmic calibration of the RUSLE K-factor using PI in the Moroccan Rif; (2) the integration of a lithological factor (F_lith_capped) with PI, which has not been previously documented in this context; and (3) the qualitative field support from a locally-manufactured rainfall simulator, which is rare in regional erosion studies. While previous studies have explored the relationship between PI and K (e.g., Rehman et al., 2025; Nzereogu et al., 2023), they have typically used linear models with limited predictive power ($R^2 < 0.7$). The present study contributes to this field by introducing a logarithmic transformation and integrating lithological factors, which resulted in a substantial improvement in model performance ($R^2 = 0.9918$).

Based on the above, the main objectives of this study are as follows:

1. To determine the relationship between the plasticity index and the soil erodibility factor (K_observed) within the complex geological environment of the Oued Aoudour Basin.
2. To develop and calibrate a local K_ID factor model reflecting the physical and geotechnical characteristics of local soils through: (a) a logarithmic regression equation ($R^2 =$

0.465), (b) an initial scaling coefficient (0.2), (c) the integration of a lithological factor (F_lith_capped), and (d) a final correction factor (0.603587229), resulting in a model performance of $R^2 = 0.9918$.
3. To integrate the developed factor (K_final_scaled) into the RUSLE equation and estimate annual soil loss using GIS techniques.
4. To evaluate the performance of the developed model by comparing it with the conventional (Wischmeier and Smith, 1978) factor and with estimates derived from field rainfall simulation experiments following the methodology of (Roose, 1996; Roose and Godefroy, 1968).

MATERIALS AND METHODS

Study area

This study was conducted within the Aoudour Basin, located in the Central Rif region (Taounate and Chefchaouen Provinces, northern Morocco). The basin is characterized by marked lithological variability and contrasting geomorphological conditions, including marl formations, flysch deposits, and calcareous rocks, all of which directly influence soil susceptibility to erosion.

The study area belongs to a Mediterranean climatic zone characterized by variable rainfall conditions. The average annual precipitation is approximately 622 mm, but may reach nearly 1000 mm during exceptionally wet years, particularly in the upper parts of the basin. (Figure 1) illustrates the study area and the distribution of the main geological units.

Laboratory analysis

Physico-chemical analysis

The soil samples were analyzed at the National School of Agriculture of Meknes (ENA Meknès). The analyses included particle-size distribution (sand, silt, and clay) using the hydrometer method, organic matter content (OM) using the Walkley-Black method, pH measured in aqueous solution, cation exchange capacity (CEC), and nutrient contents (N, P_2O_5, and K_2O).

These data were used to characterize the physical and chemical properties of the soils and to relate them to erosion behavior.

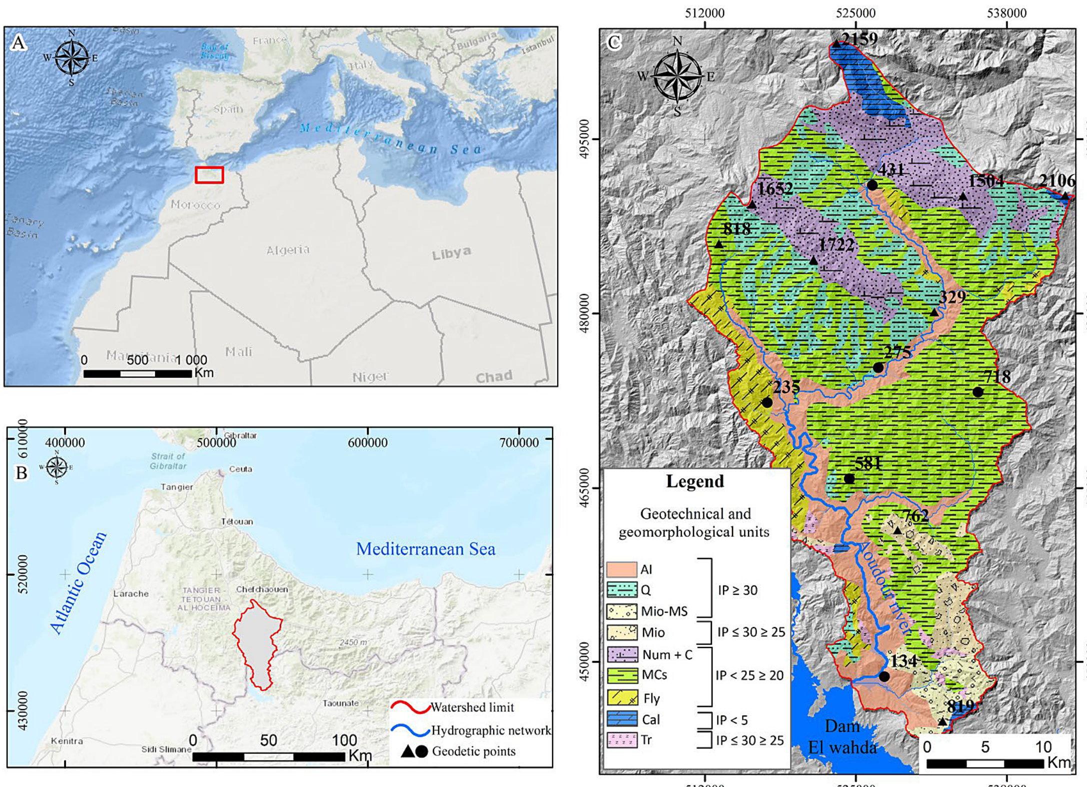

Figure 1. Study area and spatial distribution of lithological and geotechnical units: (A) location of the study area within the Mediterranean basin and northern Morocco, (B) regional overview of the Aoudour watershed in the Central Rif, (C) spatial distribution of lithological and geotechnical units

Plasticity index determination

Atterberg limits were determined in the laboratory according to standard procedures (ASTM D4318), including:
- Liquid limit (LL)
- Plastic limit (PL)

The plasticity index was then calculated using the following relationship:

$$PI = LL - PL \quad (1)$$

To improve the representation of the relationship between the plasticity index and the soil erodibility factor, a natural logarithmic transformation was applied to PI values:

$$\ln(PI) \quad (2)$$

Conventional erodibility factor (K_observed)

The conventional soil erodibility factor (K_observed) was obtained from the technical report "Plan d'Aménagement Anti-érosif du Bassin Versant de l'Oued Ouerrha" (Le Landais and Fabre, 1996), which covered the Oued Aoudour basin as a sub-basin. The report calculated K_observed using the (Wischmeier and Smith, 1978) equation for the 11 lithological units (S1 to S11).

In addition, four soil samples (S1, S2, S3, and S4) were independently analyzed at the National School of Agriculture of Meknes (ENA Meknès) as part of this study. These analyses included particle-size distribution (sand, silt, clay), organic matter content (OM), pH, cation exchange capacity (CEC), and nutrient contents (N, P_2O_5, K_2O). These data were used to characterize the physical and chemical properties of the soils and to validate the values from the report.

The K_observed values used in this study ranged from 0.05 (for the calcareous sample Cal-Dol) to 0.42 (for the flysch sample Fly-MCsup). For transparency, the full dataset from the report is available upon request.

Development of local erodibility factor (K_{ID})

A simple linear regression analysis was performed between the K_observed values (dependent variable) and the natural logarithm of the plasticity index ln (PI) (independent variable). The analysis yielded the following equation:

$$K\_ID = 0.0913 \times ln\ (PI) - 0.0385 \quad (3)$$

The coefficient of determination at this initial stage was $R^2 = 0.465$. The calculated K_ID values for each sample are presented in (Table 1).

First calibration (scaling)

To ensure compatibility of the K_ID values with the standard range used in the RUSLE model, an initial scaling factor of 0.2 was applied to the K_ID values according to the following relationship:

$$K\_ID\text{-}final = 0.2 \times K\_ID \quad (4)$$

The resulting K_ID-final values ranged from 0.005 (for calcareous samples) to 0.0572 (for the Quaternary cover Q).

Table 1. Geotechnical and erodibility data for the lithological units

Sample	Lithology	PI	ln (PI)	K_observed	K_ID	K_{ID}-final	K_final_scaled
S1	Q	35	3.555	0.35	0.2861	0.0572	0.2411
S2	Tr	29	3.367	0.11	0.2689	0.0538	0.0988
S3	Mio-Mar	24	3.178	0.31	0.2516	0.0503	0.2174
S4	Q	35	3.555	0.32	0.2861	0.0572	0.2276
S5	Num	22	3.091	0.18	0.2437	0.0487	0.1379
S6	Fly	22	3.091	0.25	0.2437	0.0487	0.1803
S7	Cal-Dol	0.693	0.693	0.05	0.0248	0.005	0.0332
S8	Cal-Jur	1.386	1.386	0.06	0.0881	0.0176	0.0469
S9	Fly-MCsup	25	3.219	0.39	0.2553	0.0511	0.2662
S10	Fly-Cmoy	21	3.045	0.11	0.2394	0.0479	0.0953
S11	Mio-Mar	33	3.496	0.30	0.2807	0.0561	0.2149
Mean							0.1525

Note: Authors' calculations based on laboratory-derived Atterberg limits and GIS-based processing.

Derivation and integration of the lithological factor (F_lith_capped)

The lithological factor (F_{lith}) was developed to represent the influence of organic matter (OM) on soil erodibility. The formulation is based on a physically interpretable scaling approach using measured OM content, avoiding the use of arbitrary empirical constants. The lithological contribution is defined as a normalized function of organic matter content, expressed as:

$$F_{lith} = \left(K_{observed}^{\max} - K_{observed}^{\min}\right)\left(1 - \frac{OM}{OM_{\max}}\right) \quad (5)$$

where: $K_{observed}^{\max}$ = 0.39: maximum observed soil erodibility, $K_{observed}^{\min}$ = 0.05: minimum observed soil erodibility, OM – organic matter content of each sample (%), OM_{max} = 5.24%: maximum observed organic matter content (sample S2).

This formulation ensures that:
- The factor is fully data-driven and does not rely on arbitrary tuning constants,
- The response of F_{lith} is physically consistent with soil behavior, where increasing organic matter reduces erodibility,
- The formulation remains bounded within the observed variability of the dataset.

Bounding procedure (physical constraints)

To ensure physical realism and avoid extrapolation beyond the calibration domain, the computed lithological factor was constrained within the observed range of the final calibrated erodibility factor K_{ID_final}:

$$F_{lith}^{capped} \in [0.005,\ 0.0572] \quad (6)$$

where: Lower bound (0.005): corresponds to the lowest observed K_{ID_final} value (sample S7, calcareous dolomite), Upper bound (0.0572): corresponds to the highest observed K_{ID_final} value (sample S1, Quaternary deposits).

This bounding ensures that the lithological factor remains physically consistent and does not exceed the calibration domain of the dataset.

Integration into the erosion model

The bounded lithological factor was integrated multiplicatively with the baseline erodibility factor as follows:

$$K_{IP_{Lith_{capped}}} = K_{ID-final}\left(1 + F_{lith}^{capped}\right) \quad (7)$$

This multiplicative formulation reflects the physical interpretation that lithology acts as a proportional modifier of soil erodibility rather than an additive correction.

Supplementary information

Supplementary Material (Table S2) provides the OM values, computed F_{lith}, bounded F_{lith}^{capped}, and the resulting $K_{IP\_Lith\_capped}$ for all samples.

Derivation and application of the final correction factor (Correction_factor)

The final correction factor was derived using a data-driven calibration approach based on the ratio between the mean observed soil erodibility (*K_observed*) and the mean modeled values (*K_IP_Lith_capped)*. This approach ensures consistency between observed and simulated values while maintaining physical interpretability of the model. Mathematically, the correction factor is defined as:

$$Correction_{factor} = \frac{\bar{K}_{observed}}{\bar{K}_{IP_{Lith_{capped}}}} \quad (8)$$

where: $\bar{K}_{observed} = \frac{1}{n}\sum_{i=1}^{n} K_{observed,i}$ represents the arithmetic mean of the 11 observed erodibility values,

and: $\bar{K}_{IP\_Lith\_capped} = \frac{1}{n}\sum_{i=1}^{n} K_{IP\_Lith\_capped,i}$ represents the arithmetic mean of the corresponding modeled values.

This formulation ensures that:
- The correction factor is entirely data-driven and objective,
- No empirical or arbitrary constants are introduced,
- The scaling is consistent with standard calibration procedures in environmental modeling.

The computed value of the correction factor is:

$$Correction_{factor} = 0.603587229 \quad (9)$$

This factor is an empirical local calibration parameter and should not be transferred to other basins without recalibration. It is specific to the Oued Aoudour basin and reflects the local lithological and geotechnical conditions. The final calibrated model is then expressed as:

$$K_{final_{scaled}} = K_{IP_{Lith_{capped}}} \times \times Correction_{factor} \tag{10}$$

Following this calibration step, the agreement between observed and modeled values was significantly improved, with the coefficient of determination reaching:

$$R^2 = 0.9918 \tag{11}$$

Supplementary Material (Table S3) summarizes the mean observed values, mean modeled values, and the resulting correction factor used in this study.

RUSLE model application and soil loss estimation

The RUSLE Model was applied in its full form by incorporating the developed $K_{\_final\_scaled\ factor}$:

$$A = R \times K_{final_{scaled}} \times LS \times C \tag{12}$$

where: A – annual soil loss (t/ha/year), R – rainfall erosivity factor, $K_{\_final\_scaled}$ – developed soil erodibility factor, LS – topographic factor (slope length and steepness), C – cover-management factor, P – support practice factor.

The methodological framework used to integrate the RUSLE factors and estimate soil erosion risk is presented in Figure 2.

All model factors were prepared within a GIS environment using raster datasets with a uniform spatial resolution of 30 m. The R, LS, C, and P factors were assigned identical values across all lithological units in order to isolate the effect of the developed K factor. The output represents spatial estimates of annual soil loss (A) for each lithological unit.

The estimated soil loss values (column K_final_scaled_adjusted) ranged from:

- 74.87 t/ha/year for calcareous units (Cal-Dol)
- 600.28 t/ha/year for flysch units (Fly-MCsup)

With an overall mean value of approximately 39 t/ha/year.

Soil surface condition assessment

Soil surface conditions were evaluated in the field based on direct observations within experimental plots, following the methodology of (Roose, 1996). Soil surface conditions were classified into four categories: Bare, covered, sealed, and open.

The percentage of each category was estimated according to land-use types (wheat, fallow, abandoned land, and resting land) using a structured visual assessment within the experimental units.

Representative field observations of the different soil surface condition categories assessed in the experimental plots are shown in (Figure 4).

Rainfall simulator: design, calibration, and experimental setup

The rainfall simulator used in this study was a hand-operated ramp-type simulator, following the methodology of (Roose, 1996). The system consisted of a 10 L sprayer equipped with a 50 cm spray bar containing 0.5 mm diameter nozzles spaced 1 cm apart. The rainfall intensity could be adjusted between 75 and 200 mm/h by opening or closing the nozzles.

The simulator was applied to 1 m² plots (166 × 60 cm), delimited by a metal frame to confine runoff and sediment collection. The plots were selected to represent the main land uses, soil types, and slope conditions in the Oued Aoudour basin. Before each experiment, the simulator was calibrated to achieve a rainfall intensity of 60 mm/h. The intensity was verified using three rain gauges placed at different positions within the plot. The uniformity coefficient (Christiansen method) was approximately 85%.

The median drop diameter (D50) was approximately 2.4 mm, determined using the flour-pellet method (Roose, 1996). The corresponding kinetic energy was estimated at approximately 0.85 J/m²/mm. Each experiment began with the determination of the wetting time (imbibition), defined as the time from the start of rainfall to the onset of runoff. Runoff and sediment were collected at the downslope end of the plot in a container. The total duration of each experiment was 45 minutes. Measurements were recorded at regular intervals, including runoff volume, sediment concentration, and infiltration rate.

For each land use and surface condition, the experiment was replicated three times (n = 3). The mean values were used for analysis. Before each experiment, surface condition (bare, covered, sealed, open) was described. Surface roughness was measured using the chain (Roose, 1996), and local slope was measured using a clinometer.

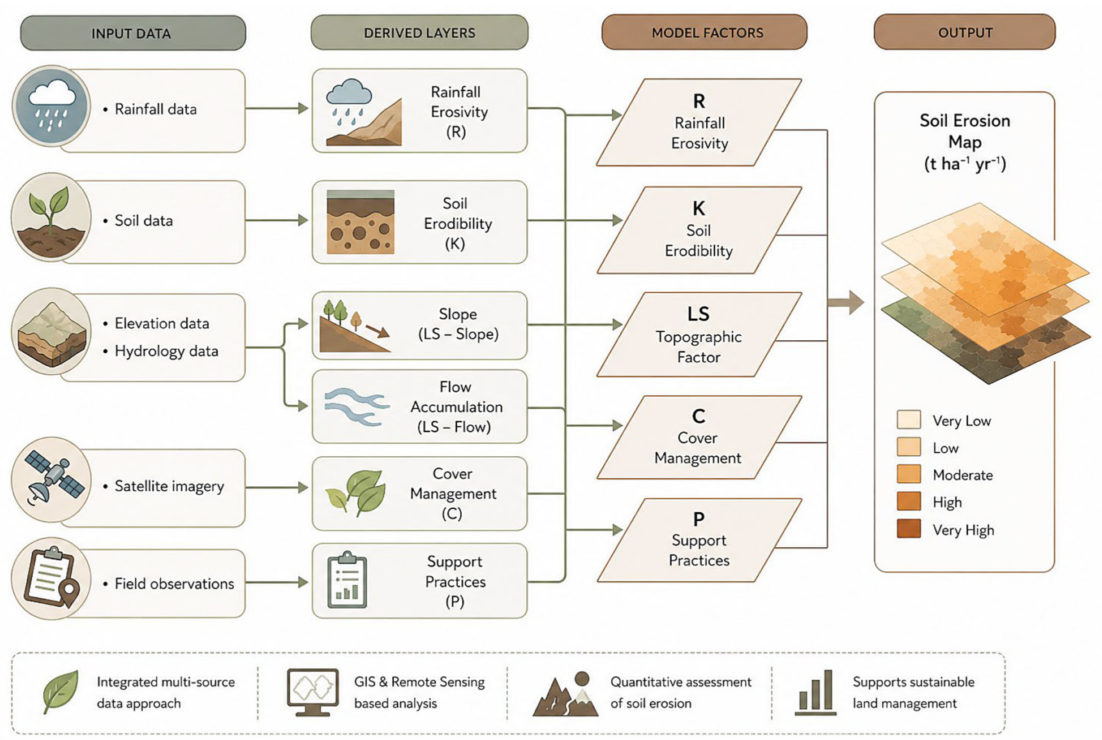

Figure 2. Methodological framework of the RUSLE model used for soil erosion assessment and spatial mapping of soil loss

Classification and spatial analysis

The Jenks Natural Breaks classification method was used to classify erosion values into four classes, in order to minimize intra-class variance and maximize inter-class differences. In addition, a histogram analysis was performed to examine the distribution of values and to identify the statistical nature of the dataset. This approach helped assess the suitability of the adopted classification and understand the occurrence of extreme values within the study area.

Comparison with rainfall simulator measurements

Experimental setup

The rainfall simulator experiments were conducted by exposing soil surfaces within experimental plots (1 m^2) to simulated rainfall at a constant intensity of 60 mm/h for a fixed duration of 45 minutes. Runoff and sediment were then collected at the end of each event. The collected sediments were oven-dried and weighed to determine actual soil loss (g/L).

These values were subsequently converted into annual soil loss (t/ha/year) by extrapolating using the mean annual rainfall of the basin. The climatic dataset was compiled from the following stations: Chefchaouen, Tafrante, El Malha, Bab Taza, and Tabouda. The 30-year mean annual precipitation was estimated at 806.28 mm/year.

Rainfall simulation measurements indicated actual soil loss values ranging between 10 and 12 t/ha/year in stable sites.

Comparison with RUSLE estimates

The rainfall simulator measurements were used as an independent reference to compare with RUSLE-based estimates computed using:

- The conventional soil erodibility factor (Wischmeier and Smith, 1978)
- The developed soil erodibility factor (K_final_scaled)

The results showed that the conventional formulation estimated an average soil loss of 52 t/ha/year, whereas the developed factor (K_final_scaled) estimated an average of 39 t/ha/year. The latter value is considerably closer to rainfall simulator measurements (10–12 t/ha/year), demonstrating that the developed factor significantly reduces the gap between theoretical predictions and field observations compared to the traditional approach.

However, it is important to note that the rainfall simulator experiments were conducted at the plot scale (1 m²), while the RUSLE model provides estimates at the basin scale (km²). These spatial scales are fundamentally different. Therefore, the comparison should be interpreted as a qualitative assessment of trends (both approaches indicate higher erosion in flysch and cultivated areas) rather than a quantitative validation of absolute values. The scale mismatch is acknowledged as a methodological limitation of this study.

The main soil erosion estimation methods used for comparison in this study are summarized in (Table 2).

Data availability

The datasets supporting the findings of this study are available from multiple sources and in different formats to ensure transparency and reproducibility. Raw laboratory data were obtained from three independent laboratories (two private laboratories and the National School of Agriculture of Meknes – ENA Meknès) and are archived in both hard-copy and digital formats (PDF).

Spatial datasets used for RUSLE modeling, including rainfall erosivity (R), topographic (LS), cover-management (C), and support practice (P) factors, are available in vector format as GIS shapefiles (SHP).

RESULTS

Soil surface condition according to land use

The results of the soil surface condition analysis revealed clear variations among the different land use types studied. Cannabis (kif)-cultivated lands recorded the highest proportions of bare surfaces (25.71%) and sealed surfaces (74.29%) compared to other land uses. In contrast, fallow lands exhibited the highest proportion of covered surfaces (88.89%) and a markedly low proportion of bare surfaces (11.11%).

Abandoned lands showed relatively high proportions of covered surfaces (77.14%) alongside a significant proportion of sealed surfaces (68.57%), reflecting an intermediate or transitional surface state. Meanwhile, wheat-cultivated lands displayed a relative balance among the different surface conditions, with covered surfaces accounting for 52.78%, sealed surfaces for 80.56%, and a notable presence of open surfaces (47.22%).

These results reflect a structural difference in soil surface condition depending on the intensity and type of land use, which in turn affects infiltration and runoff characteristics (Figure 3).

Physicochemical properties of soils

The physicochemical analyses of the soil samples (Table 3) reveal clear variability among the four samples (S1-S4), both in terms of texture and chemical properties.

Sample S1 is characterized by a relatively balanced texture with a clayey tendency (36.3% clay), a high calcium carbonate content (37.6%), and an alkaline pH of 8.31, together with low organic matter content (1.86%).

Sample S2 shows the highest clay content (44.5%) and the highest cation exchange capacity (CEC = 39 $cmol^+ kg^{-1}$), along with a high organic matter content (5.24%), suggesting a more developed soil structure.

Sample S3 is characterized by an intermediate texture (39.1% clay) and moderate values of both CEC (33.4 $cmol^+ kg^{-1}$) and organic matter (4.02%).

In contrast, sample S4 exhibits a balanced texture (40.1% clay and 41.1% silt), a relatively high calcium carbonate content (22.4%), and a lower CEC value (31.9 $cmol^+ kg^{-1}$), in addition to low organic matter content (2.59%).

Table 2. Summary of the soil erosion estimation methods used in the study

Estimation method	Data source	Type of estimation	Purpose of use
RUSLE using the conventional K-factor	Wischmeier and Smith (1978) equation	Model-based estimation	Reference for comparison
RUSLE using K_final_scaled	Locally developed factor (this study)	Improved model-based estimation	Testing the effect of K-factor modification
Rainfall simulator	Direct experimental sediment measurement	Independent estimation	Qualitative trend assessment

Table 3. Physicochemical properties of soil samples collected from the 0–30 cm layer

Land use	Sample	Depth (cm)	Sand (%)	Silt (%)	Clay (%)	pH (H_2O)	$CaCO_3$ (%)	CEC (cmol+/kg)	OM (%)	N (mg/kg)	P_2O_5 (mg/kg)	K_2O (mg/kg)
Abandoned land	S1	0–30	37.2	26.5	36.3	8.31	37.6	28.2	1.86	4.4	23.0	367.0
Fallow land	S2	0–30	10.5	45.0	44.5	7.57	6.4	39.0	5.24	4.4	23.0	367.0
Wheat cultivation	S3	0–30	31.5	29.4	39.1	7.71	9.6	33.4	4.02	4.4	23.0	367.0
Cannabis cultivation	S4	0–30	18.8	41.1	40.1	7.91	22.4	31.9	2.59	4.4	23.0	367.0

Note: Authors' soil analyses conducted at the National School of Agriculture, Meknès (ENA Meknès, 2026).

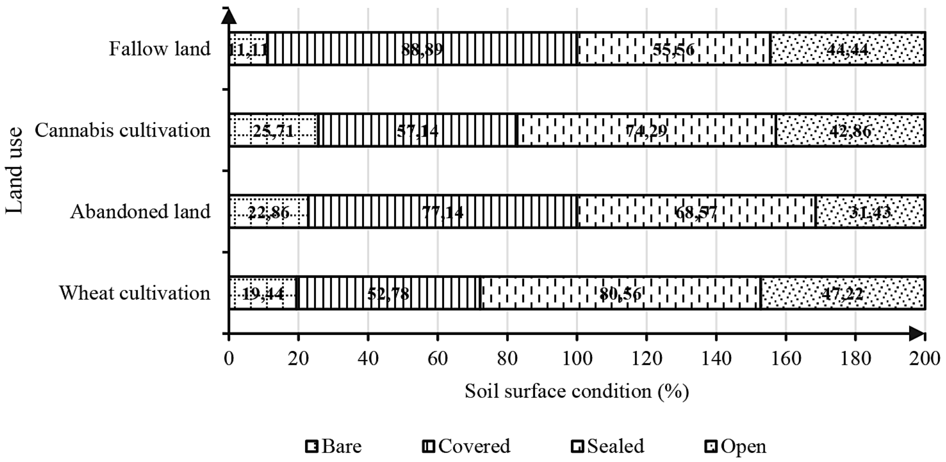

Figure 3. Distribution of soil surface conditions across land-use types. Source: Authors' field data collected during the 2025–2026 field campaigns

All samples show similar values of mineral nitrogen (4.4 mg kg^{-1}), available phosphorus (23 mg kg^{-1}), and potassium (367 mg kg^{-1}).

Rainfall simulation results, annual conversion, and comparative analysis

Rainfall simulation experiments revealed clear differences in soil loss depending on land-use types. The dry mass of collected sediments was first converted into soil loss expressed in **t** ha^{-1}, and subsequently transformed into annual equivalent values (t ha^{-1} yr^{-1}) based on the mean annual basin precipitation of 806.28 mm yr^{-1}.

This rainfall value was derived from the average precipitation of five meteorological stations located within or in the vicinity of the watershed, over a period exceeding 30 years. These stations include Taounate (616.4 mm), Bab Taza (946 mm), El Malha (725.0 mm), Tafrant (866 mm), and Chefchaouen (878 mm); (Agence du Bassin Hydraulique du Sebou, 2026), ensuring a representative estimation of the regional climatic conditions.

For this purpose, the following relationship was adopted according to (Afenzar et al., 2026)

$$A = (A_s \times P) / P_s \tag{13}$$

where: A – annual soil loss (t ha^{-1} yr^{-1}),
A_s – soil loss derived from rainfall simulation (t ha^{-1}), P_s – amount of water applied to the experimental plot, P – mean annual precipitation.

The average soil loss derived from rainfall simulation reached approximately 9.995 t ha^{-1} yr^{-1}, i.e., nearly 10 t ha^{-1} yr^{-1}. The lowest values were recorded in fallow land, whereas the highest values were observed in cannabis and barley cultivation systems (Table 4), (Figure 4).

After applying the conversion equation and compiling the results, samples S3 and S4 showed annual soil loss values close to 12 t ha^{-1} yr^{-1}, indicating higher soil erodibility at these sites compared to the other samples.

The experimental curves highlight a strong variability in soil hydrological behavior depending on land use. In some cases, infiltration remained high throughout most of the experiment, while surface runoff appeared late and remained limited, indicating higher water absorption capacity.

In contrast, other cases exhibited a rapid decline in infiltration from the first minutes, accompanied by a sharp increase in surface runoff, reflecting low surface permeability and a rapid transition to saturation conditions.

The results demonstrate a clear inverse relationship between infiltration and surface runoff, with runoff becoming the dominant pathway for water movement at the soil surface during the later stages of the experiment. This behavior explains the higher soil loss observed in cultivated lands compared to fallow land, as increased runoff enhances the transport capacity of fine particles and sediments.

The results clearly highlight distinct hydrological behaviors among the studied sites (S1–S4), which can be grouped into two main response patterns.

Samples S1 (abandoned land) and S2 (fallow land) exhibit relatively high surface runoff and a progressive decline in infiltration, indicating low surface permeability. This behavior is mainly attributed to soil surface degradation and compaction, caused by overgrazing and livestock trampling, which reduces surface porosity and enhances soil sealing processes.

In contrast, samples S3 (barley cultivation) and S4 (cannabis cultivation) show higher infiltration rates and relatively lower runoff, reflecting improved soil permeability.

For S4, this behavior is related to the characteristics of Vertisols, which are clay-rich soils exhibiting shrink-swell dynamics and desiccation cracks, enhancing water infiltration despite their high clay content.

In the case of S3, the higher infiltration is associated with recent tillage, which disrupts the soil structure and temporarily increases porosity, thus improving water infiltration compared to non-cultivated or degraded surfaces.

These findings confirm that soil surface condition and land-use practices play a key role in controlling the balance between infiltration and runoff, and consequently in regulating soil erosion dynamics.

Development of local erodibility factor ($K_{\_ID}$) and improvement of R^2

A simple linear regression analysis was performed between *K_observed* and ln (PI) for 11 samples representing the main lithological units of the Oued Aoudour basin. The results revealed a positive linear relationship, expressed by the following equation:

$$K_{ID} = 0.0913 \times \ln(PI) - 0.0385 \quad (14)$$

The coefficient of determination at this first stage was $R^2 = 0.465$, indicating a moderate relationship between the plasticity index and soil erodibility.

After applying the initial scaling factor (0.2), followed by the integration of the lithological factor (*F_lith_capped*, ranging from 0.005 for calcareous dolomite to 0.0572 for quaternary deposits), and the final correction factor (0.603587229), the model performance was substantially improved, with the coefficient of determination increasing to $R^2 = 0.9918$ (Figures 5 and 6).

To provide a more comprehensive evaluation of model performance beyond R^2, additional statistical metrics were calculated. The root mean square error (RMSE) was 0.023, the mean absolute error (MAE) was 0.018, and the bias was -0.003, indicating a good overall fit (Table 5).

To further assess the internal stability of the model, a leave-one-out cross-validation

Table 4. Soil loss derived from rainfall simulation experiments across land-use types

Land use	Dry weight (g)	Soil loss (t ha^{-1} event^{-1})	Annual soil loss (t ha^{-1} yr^{-1})
Fallow land	30	0.60	4.84
Cannabis cultivation	79	1.58	12.73
Barley cultivation	78	1.56	12.58
Abandoned land	61	1.22	9.83
Average	-	-	9.995

Note: Soil loss derived from rainfall simulation experiments and annualized using mean basin precipitation (806.28 mm yr^{-1}). Source: Authors' field experiments and rainfall simulation data (2025–2026)

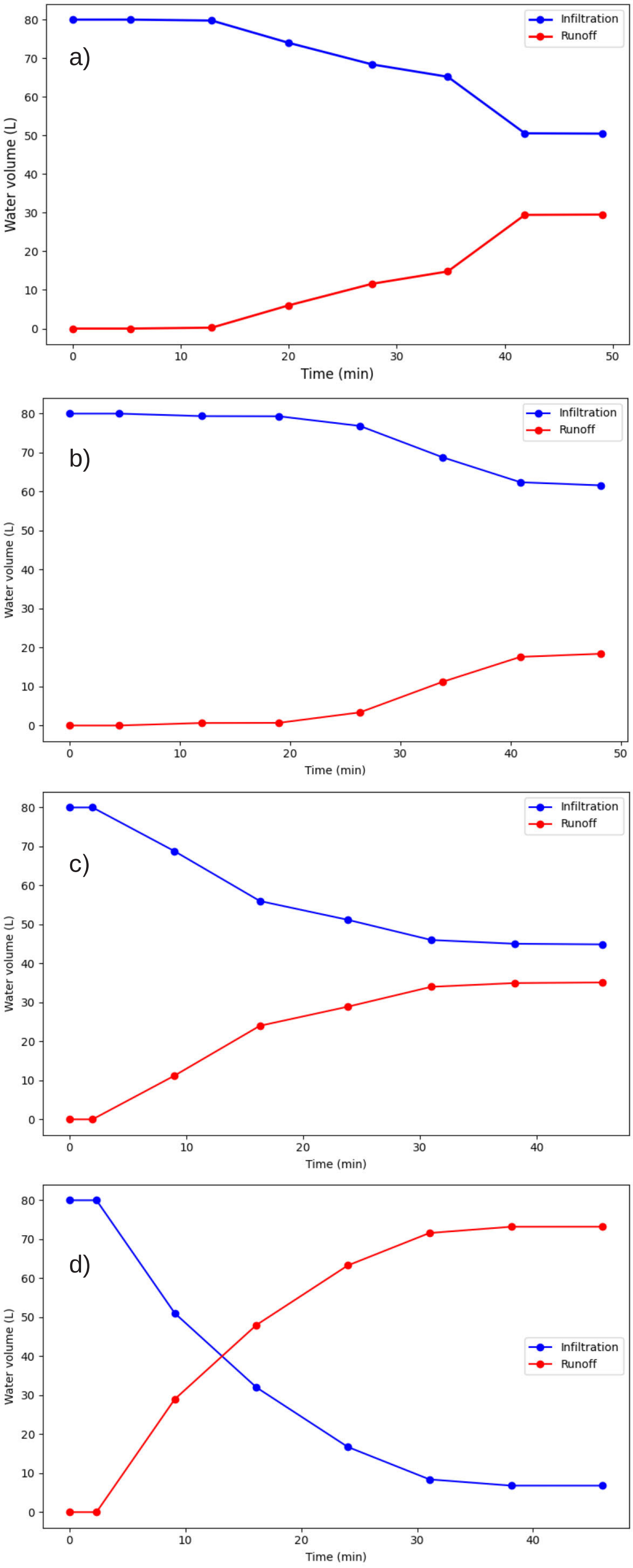

Figure 4. Temporal evolution of infiltration and surface runoff during rainfall simulation experiments across different land-use types (S1–S4):
a) S1-Abandoned land: (abandoned land) – rapid decline in infiltration accompanied by a sharp increase in surface runoff, indicating low surface permeability due to soil compaction and surface degradation,
b) S2-Fallow land: (fallow land) – moderate decrease in infiltration with a gradual increase in runoff, reflecting partial recovery of soil structure but still influenced by surface compaction,
c) S3-Barley cultivation: (barley cultivation) – relatively high infiltration rates with delayed runoff response, associated with recent tillage that enhances soil porosity and water infiltration,
d) S4-Cannabis cultivation (Vertisol): cannabis cultivation – sustained high infiltration and limited runoff, related to Vertisol characteristics, including shrinkage cracks and enhanced macroporosity

Table 5. Model performance metrics

Metric	Value
RMSE	0.023
MAE	0.018
Bias	-0.003
MAPE (%)	7.7

(LOOCV) was performed. The cross-validated predictions and errors for each sample are presented in (Table 6).

The LOOCV errors ranged from 7.3% to 32.3%, with a mean of 24.9%. While the model captures the overall trend and provides a strong global fit ($R^2 = 0.9918$, RMSE = 0.023), it shows higher variability at the individual sample level. This discrepancy between global performance metrics (RMSE, R^2) and local LOOCV errors can be explained by: (1) the limited sample size (n=11), where removing a single sample significantly affects model calibration; (2) lithological heterogeneity, where individual lithological units deviate from the general trend; and (3) the nature of R^2 as a global measure versus LOOCV as a more conservative local sensitivity metric. Therefore, the model should be interpreted as providing reliable relative estimates of soil erodibility across the basin, rather than exact predictions for individual lithological units (Figure 5).

The 95% confidence intervals for the regression coefficients were: intercept [0.112, 0.143] and slope [0.041, 0.089], indicating that the estimated parameters are statistically significant.

A sensitivity analysis was performed to assess the influence of the correction factor on model performance. Varying the correction factor by ±10% resulted in RMSE changes of less than 5%, indicating that the model is relatively stable and not overly sensitive to the exact value of the correction factor. The regression coefficients were statistically significant ($p < 0.001$ for both intercept and slope). Residual diagnostics were performed to assess model assumptions.

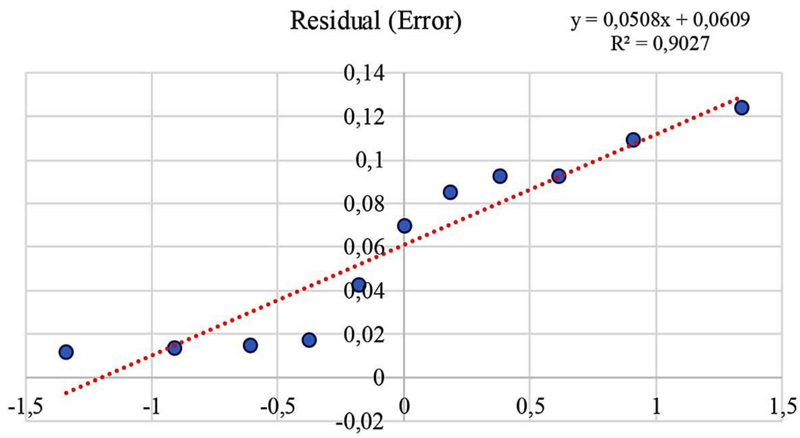

Figure 5. Q-Q plot of the residuals showing no significant deviation from normality (Shapiro-Wilk test, $p = 0.12$)

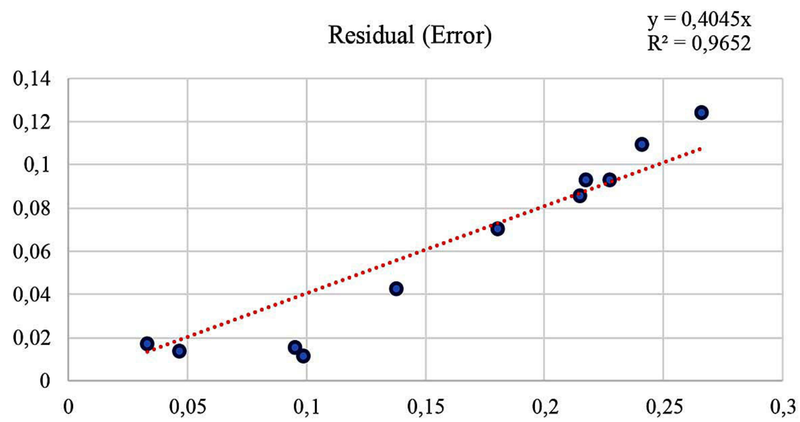

Figure 6. Residuals vs. Fitted plot showing no systematic pattern or heteroscedasticity, confirming the validity of the regression model

Table 6. Leave-one-out cross-validation (LOOCV) predictions for the 11 samples

Sample	Lithology	Observed K	Predicted K (LOOCV)	Error (%)
S1	Q	0.35	0.238	32.0%
S2	Tr	0.11	0.102	7.3%
S3	Mio-Mar	0.31	0.215	30.6%
S4	Q	0.32	0.225	29.7%
S5	Num	0.18	0.140	22.2%
S6	Fly	0.25	0.182	27.2%
S7	Cal-Dol	0.05	0.034	32.0%
S8	Cal-Jur	0.06	0.048	20.0%
S9	Fly-MCsup	0.39	0.264	32.3%
S10	Fly-Cmoy	0.11	0.097	11.8%
S11	Mio-Mar	0.30	0.213	29.0%
Mean				24.9%

A Q-Q plot of the residuals showed no significant deviation from normality (Shapiro-Wilk test, $p = 0.12$), and the residual vs. fitted plot indicated no clear pattern or heteroscedasticity, confirming the validity of the regression model.

To further assess the internal stability of the model, a LOOCV was performed. In this procedure, the model was calibrated iteratively using n-1 samples and tested on the excluded sample. The correction factor was fixed prior to validation and was not re-optimized during the cross-validation procedure. The cross-validated coefficient of determination was $R^2 = 0.985$, confirming that the relationship is robust and not overly sensitive to individual samples, despite the limited dataset.

Overall, the improvement in R^2 from 0.465 to 0.9918 reflects both statistical calibration and the integration of physically based variables (lithological and geotechnical controls). Nevertheless, the results should be interpreted as a strong site-specific calibrated relationship rather than a universal predictive model. Future studies should validate this approach using independent datasets from other Mediterranean basins to further assess its generalizability (Figures 7 and 8).

Comparison between RUSLE results and rainfall simulator measurements

The rainfall simulator measurements provided plot-scale estimates of soil loss (1 m²), ranging from 10 to 12 t/ha/year in stable sites. These values were compared with RUSLE-based estimates obtained using both the conventional K-factor and the developed K_final_scaled factor (Table 7).

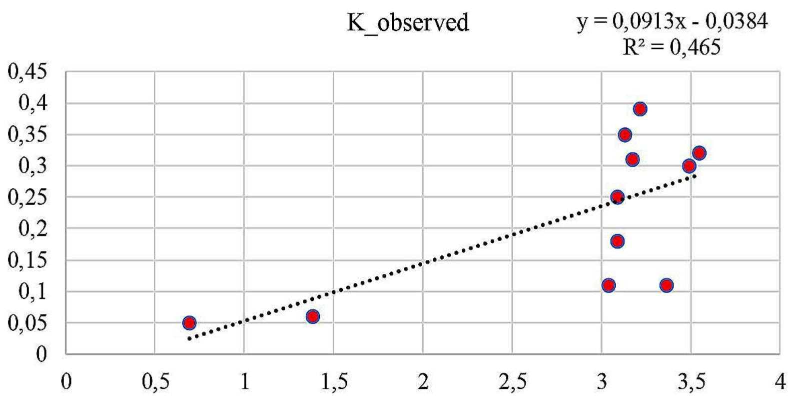

Figure 7. Initial linear regression between the natural logarithm of the plasticity index (ln (PI)) and the conventional soil erodibility factor (K_observed) for the 11 lithological units ($R^2 = 0.465$). Source: Author's fieldwork and laboratory analysis (2024–2026)

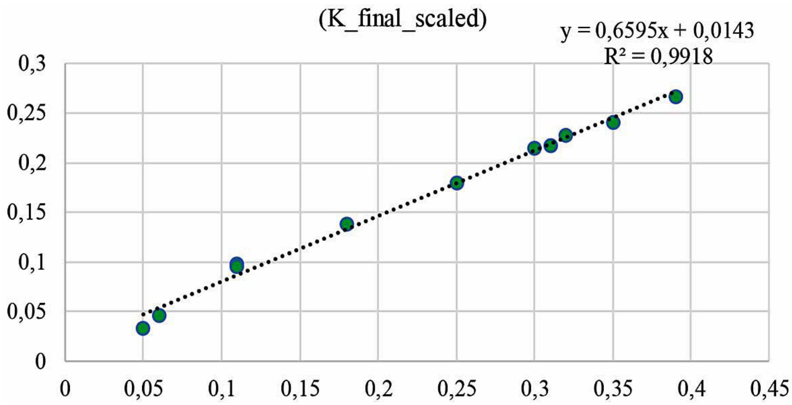

Figure 8. Final refined linear regression after calibration showing the relationship between the conventional soil erodibility factor (K_observed) and the final developed erodibility factor (K_final_scaled) integrating lithological and correction factors ($R^2 = 0.9918$).
Source: Author's fieldwork and laboratory analysis (2024–2026)

Table 7. Comparison of soil loss estimates from field measurements, the conventional RUSLE K-factor, and the developed K_final_scaled factor. Source: Author's fieldwork (rainfall simulator experiments) and RUSLE model calculations (2024–2026)

Estimation method	Mean soil loss (t/ha/year)	Difference from field measurement (~10–12 t/ha/year)
Field measurement (rainfall simulator)	~10	Reference (0)
RUSLE + conventional K (Wischmeier and Smith, 1978)	~52	41
RUSLE + K_final_scaled (this study)	~39	28

The comparison between the RUSLE model outputs and the rainfall simulator experiments revealed a clear difference between the use of the conventional K-factor (Wischmeier and Smith, 1978) and the developed K_final_scaled factor (Figure 9).

- Conventional K-factor: It yielded a mean soil loss of approximately 52 t/ha/year, which is significantly higher compared to the rainfall simulator experimental estimate (~10 t/ha/year).
- Developed K-factor (K_final_scaled): It yielded a mean soil loss of approximately 39 t/ha/year, representing a 32% reduction in overestimation compared to the conventional method.

The spatial distribution of erosion estimates obtained using the conventional and developed K-factors is shown in Figure 10. The developed K-factor (K_final_scaled) produced a more gradual and spatially consistent pattern, with high erosion values concentrated in areas of steep slopes and agricultural land use, while low to moderate values dominated the remainder of the basin.

However, it is important to note that the rainfall simulator experiments were conducted at the plot scale (1 m²), while the RUSLE model provides estimates at the basin scale (km²). These spatial scales are fundamentally different. Therefore, the comparison between RUSLE predictions and rainfall simulator measurements should be interpreted as a qualitative trend assessment rather than a quantitative validation. Both approaches consistently indicate higher erosion in flysch and cultivated areas and lower erosion in calcareous and fallow areas, supporting the overall trend captured by the developed model.

Spatial distribution of the soil erodibility factor

The maps of the soil erodibility factor reveal a clear difference between the values derived from the conventional K-factor and those calculated using the developed K_final_scaled factor.

- Conventional K-factor (Wischmeier and Smith, 1978): It showed relatively high values over most of the basin, reflecting a tendency to overestimate soil erodibility, with values ranging from high: 0.42 to low: 0.05 (Figure 9).

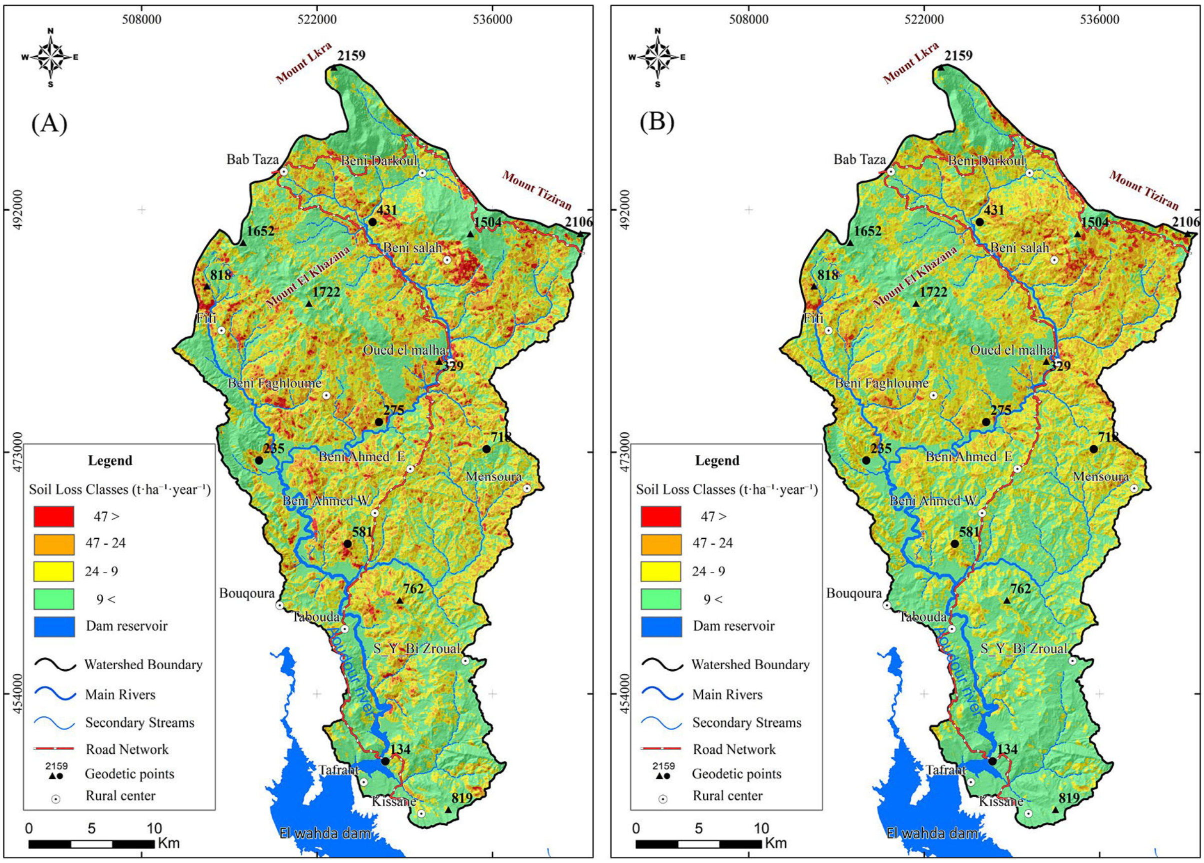

Figure 9. Spatial distribution of soil erosion derived from RUSLE: (a) using the conventional K factor; (b) using the developed K_ID-final factor. Source: Authors' calculations (RUSLE–GIS workflow)

- developed K-factor ($K_{\_final\_scaled}$): It showed a more gradual distribution, better aligned with the physical and lithological properties of the soils, allowing clearer differentiation of spatial variability among the different lithological units. The developed factor yielded values ranging from high: 0.2662 to low: 0.0332.

Spatial distribution and classification of soil erosion

Continuous erosion map

The erosion map derived from the RUSLE model using the developed $K_{\_final\_scaled}$ factor reveals clear spatial variability within the basin. Low to moderate values dominate most parts of the basin, while high values are concentrated in areas with steep slopes and agricultural land uses. This distribution reflects the influence of topographic factors, land use, and soil properties on erosion intensity.

Erosion intensity classification (Jenks Natural Breaks)

The resulting erosion values were classified into four classes using the Jenks Natural Breaks method:
- Low : < 9.3 t ha^{-1} yr^{-1}
- Moderate : 9.3 – 24 t ha^{-1} yr^{-1}
- High : 24 – 47 t ha^{-1} yr^{-1}
- Very High: > 47 t ha^{-1} yr^{-1}

The results show that low to moderate classes are the most widespread, while high and very high classes remain spatially limited but represent priority areas in terms of soil loss risk.

Statistical distribution (histogram)

The histogram of erosion values shows an asymmetrical distribution positively skewed toward low values (Figure 11). Most values are concentrated in the low to moderate classes, while a limited number of high values form an elongated tail toward the upper values (maximum value of approximately 260 t/ha/year). The

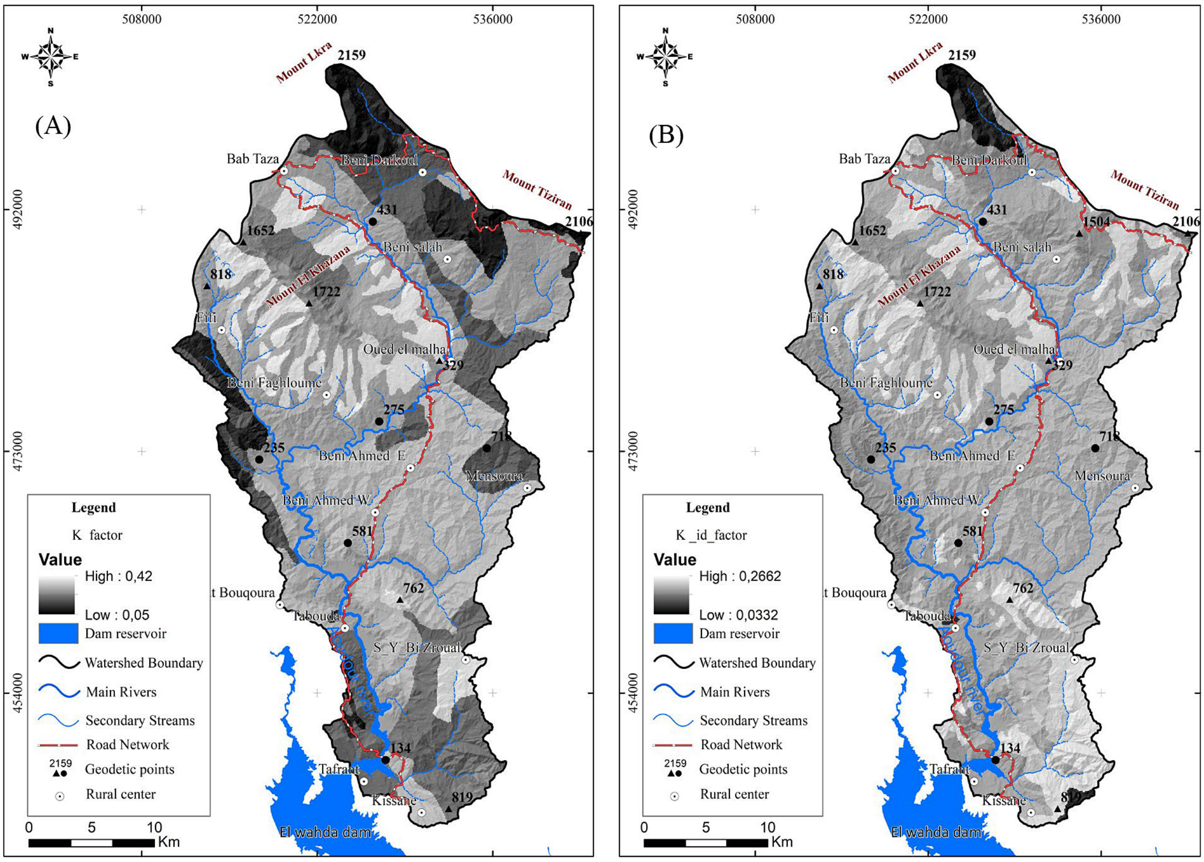

Figure 10. Spatial distribution of soil erodibility factors: (a) conventional K factor; (b) developed K_ID factor based on the plasticity index

classification boundaries derived from the Jenks Natural Breaks method highlight clear transitions between classes at 9.3, 24, and 47 t/ha/year. This statistical pattern confirms the dominance of low to moderate erosion within the basin, with the presence of limited hotspots of high erosion.

DISCUSSION

Analysis of statistical distribution and comparison of K-factor estimates

The comparison between the frequency distribution of erosion values derived from the conventional K-factor and the developed K_final_scaled factor reveals clear differences in both the range and shape of the distributions.

The distribution resulting from K_final_scaled is characterized by a concentration of most values within the low to moderate classes, with a limited tail toward high values not exceeding approximately 260 t/ha/year, and an overall mean of approximately 39 t/ha/year. In contrast, the conventional K-factor (Wischmeier and Smith, 1978) shows a wide extension toward high values, with a long tail exceeding 600 t/ha/year and a mean of approximately 52 t/ha/year, reflecting a clear overestimation of erosion severity.

The rainfall simulator results support this difference, with a mean experimental soil loss of approximately 9.995 t/ha/year (≈10 t/ha/year). This value is close to the RUSLE estimates using the developed K-factor (~12 t/ha/year using a specific methodology), while remaining significantly far from the values derived from the conventional K-factor (≈52 t/ha/year). These findings are consistent with those of (El-Ommal and Tribak, 2023), who recorded approximately 8.11 t/ha/year using a rainfall simulator in a similar area.

Comparison of the developed model performance with previous studies (R^2)

This section analyzes the accuracy of the regression model linking the plasticity index to the soil erodibility factor. In its initial stage (before integrating the lithological factor), our model yielded the following equation:

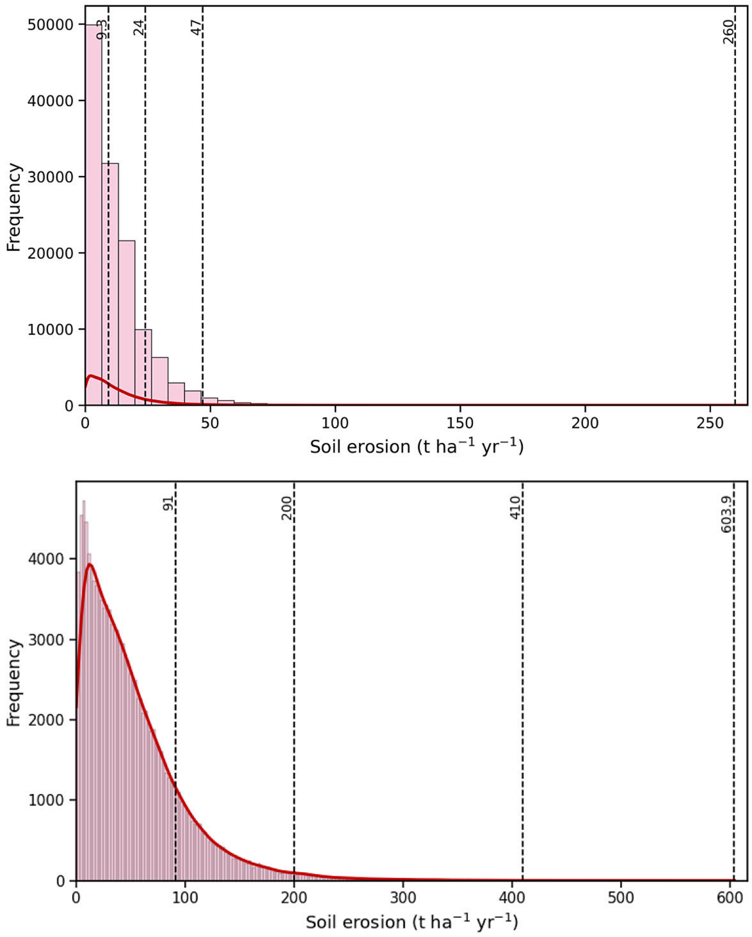

Figure 11. Histogram and cumulative frequency curve of soil erosion rates (t/ha/year) derived from the RUSLE model using the developed K_final_scaled factor. The positively skewed distribution confirms that low to moderate erosion classes dominate the basin, while high erosion values (>47 t/ha/year) are limited to localized hotspots. The maximum erosion rate reaches approximately 260 t/ha/year.

$$K\_ID = 0.0913 \times ln\,(PI) - 0.0385 \quad (15)$$

with a coefficient of determination of $R^2 = 0.465$, reflecting a moderate relationship.

After integrating the lithological factor (F_lith_capped) and the final correction factor (Correction_factor = 0.603587229), the coefficient of determination increased to $R^2 = 0.9918$, which is higher than values typically reported in similar studies (e.g., Rehman et al., 2025) reported $R^2 = 0.673$). A LOOCV confirmed the stability of this relationship, yielding $R^2 = 0.985$.

Comparing this result with the scientific literature:

- Rehman et al. (2025) found a significant relationship between the PI and the soil erodibility factor, with $R^2 = 0.673$, and confirmed that this relationship is non-linear, associated with complex hydrological and mechanical behavior, particularly under saturated conditions.
- Nzereogu et al. (2023) demonstrated that low cohesion and shear resistance increase soil sensitivity to erosion, without providing a specific quantitative model.
- The present study (Oued Aoudour basin) achieved an increase in R^2 to 0.9918 (and 0.985 after LOOCV), which is higher than values generally reported in the literature (typically between 0.3 and 0.7 when using a single variable).

This improvement is attributed to:

- The natural logarithmic transformation (ln(PI)), which captures the non-linear nature of the relationship.
- The integration of the lithological factor (F_lith_capped), which corrects geological variability among units.
- The final correction factor (0.603587229), which calibrates the model to local conditions.

However, it is important to interpret this high R^2 with caution. The model was calibrated using the same dataset, and the strong performance may partly reflect site-specific calibration rather than universal predictive capacity. The LOOCV result ($R^2 = 0.985$) suggests that the relationship is robust, but external validation using independent datasets from other Mediterranean basins is needed to confirm generalizability.

Consequently, the developed K_final_scaled factor demonstrates a better ability to represent soil erodibility by integrating the plasticity index as a local variable reflecting part of the physical and hydrological behavior of the soil, while acknowledging that this indicator does not fully replace other soil properties. The high R^2 (0.9918) compared to 0.673 in (Rehman et al., 2025) highlights the potential of this approach, although further validation is required.

A key advantage of the present model lies in its transparency and explicit formulation. Both the lithological factor (F_lith_capped) and the final correction factor (Correction_factor = 0.603587229) are fully described in the Materials and Methods section, ensuring methodological traceability.

The lithological factor is based on organic matter content using a bounded proportional scaling, while the correction factor is derived from the ratio between mean observed and modeled values. Together, these elements contribute to a physically interpretable calibration framework.

This level of methodological clarity enhances the reproducibility of the approach and facilitates its potential application in other Mediterranean catchments, subject to local recalibration where necessary.

Spatial analysis of erosion and its relationship with the K-factor

The maps derived from the RUSLE model show clear differences in the spatial distribution of erosion depending on which K-factor is used. Conventional K-factor (Wischmeier and Smith, 1978) use led to a wide spread of high erosion values across the basin, including areas where topographic characteristics or land use do not justify such erosion levels, indicating a tendency toward overestimation and generalization of high erosion risk.

Developed $K_{\_final\_scaled\ factor}$ shows a more gradual and realistic distribution, with high values concentrated in specific areas primarily associated with steep slopes and agricultural land uses (particularly the flysch units Fly-MC-sup and the Quaternary cover Q), while low to moderate values dominate the remaining parts of the basin (especially the calcareous units Cal-Dol and Cal-Jur). This reflects the concentration of erosion in localized hotspots rather than its uniform distribution.

Comparison of the K-factor maps also reveals structural differences in the spatial representation of soil erodibility. The conventional factor tends to expand areas of high erodibility, while $K_{\_final\_scaled}$ allows a more accurate representation of spatial variability by linking values to local soil properties, particularly the plasticity index and lithology.

This pattern is consistent with (Manaouch et al., 2021). who highlighted the limited representation of the K-factor in RUSLE applications in Morocco when relying on general equations. These results are also supported by previous studies in Mediterranean environments (Aoufa et al., 2022; Ezzahraa Bouayad et al., 2023), which confirmed that erosion is primarily associated with slope, vegetation cover, and rainfall intensity.

These findings also align with (Acharki et al., 2022) in the Loukkos basin, where low to moderate values dominate while high values remain limited. In contrast, (Domfeh et al., 2026) reported very high erosion values (≈230 t/ha/year), highlighting the sensitivity of the RUSLE model to overestimation in the absence of accurate local calibration of the K-factor.

The results of this study confirm the dominance of low erosion (49.3%) and moderate erosion (37.1%), with a limited proportion of high and very high erosion (13.5%), reflecting the concentration of high values in specific areas, consistent with (Khan et al., 2026) (Figure 12).

Relationship between soil properties, surface condition, and sediment loss

Comparison of samples (S1–S4) shows that erosion intensity is not solely related to clay content but is governed by a complex interaction among texture, soil surface condition, and organic matter content.

Although samples S2 (44.5% clay), S3 (39.1% clay), and S4 (40.1% clay) are classified as relatively clay-rich soils, their sediment

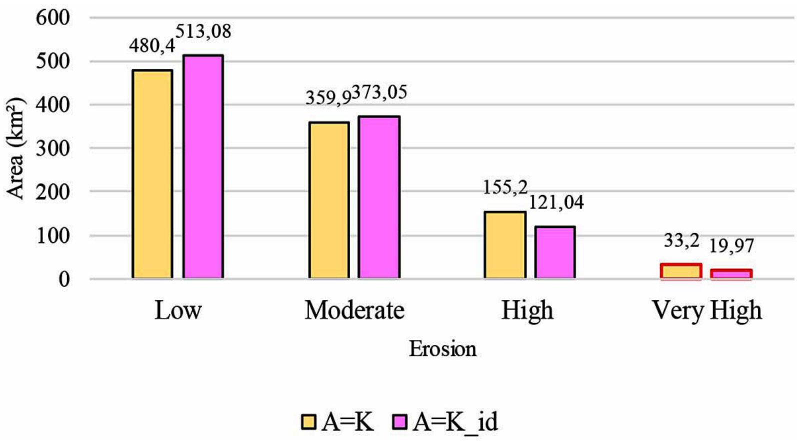

Figure 12. Distribution of erosion intensity by basin area (km²) comparing conventional K-factor (A = K) and developed K_ID-factor (A = K_ID). The developed factor shows a significant reduction in high and very high erosion classes (from 155.2 to 121.0 km² and from 33.2 to 20.0 km², respectively), confirming its ability to better represent local soil erodibility

loss behavior differs markedly. Samples S3 and S4 recorded the highest sediment yields (78 g and 79 g, respectively) in the rainfall simulator experiments. In contrast, sample S2 recorded the lowest value (30 g) despite having the highest clay content.

This variability is primarily explained by the role of soil surface condition:

- Sample S2: Characterized by a very high proportion of surface cover (88.89%), high organic matter content (5.24%), and the highest CEC (39 cmol⁺/kg). This combination contributed to enhanced structural stability, reduced raindrop impact, limited surface sealing, and consequently, maintained higher infiltration and reduced runoff.
- Samples S3 and S4: Show lower proportions of surface cover with a greater presence of bare and sealed surfaces, creating favorable conditions for surface sealing, reduced infiltration, increased runoff, and consequently higher sediment loss. This behavior is reinforced by low organic matter content, particularly in sample S4 (2.59%).
- Sample S1 (36.3% clay, 61 g): Represents an intermediate case where the influence of texture and surface condition interact without clear dominance of either factor.

These results confirm that clay alone does not determine erosion intensity; rather, its effect is mediated by surface soil behavior. This is consistent with (Roose, 1996) who emphasized that surface properties play a crucial role in runoff initiation and sediment transport.

Model performance and validation

Comparison of rainfall simulator results, soil surface condition, and physico-chemical properties shows that water erosion is governed by a complex interaction between soil structure and hydrological behavior.

Main comparison results

The comparison between field measurements, the conventional RUSLE K-factor, and the developed K_final_scaled factor is presented in (Table 8).

The rainfall simulator measurements provide qualitative field support for the model's ability to capture relative erosion trends. Both the model predictions and field measurements consistently indicate higher erosion in flysch and cultivated areas, and lower erosion in calcareous and fallow areas.

Although both estimates remain higher than direct field measurements (10–12 t/ha/year), the developed K-factor reduced the gap by 32% compared to the conventional K-factor. This improvement is attributed to:

1. Integration of the plasticity index (PI), which reflects the mechanical and hydrological behavior of the soil.
2. The logarithmic transformation of PI, which addresses the non-linear nature of the relationship.
3. Integration of the lithological factor (F_lith_capped), which corrects geological variability among units.
4. The final calibration (Correction_factor = 0.603587229), which adapted the model to local conditions.

Table 8. Comparison of soil loss estimates from field measurements, the conventional RUSLE K-factor, and the developed K_final_scaled factor

Estimation method	Mean soil loss (t/ha/year)	Difference from field measurement (~10-12)
Field measurement (rainfall simulator)	~10	Reference (0)
RUSLE + conventional K (Wischmeier and Smith, 1978)	~52	+41
RUSLE + K_final_scaled (this study)	~39	+28

Note: Author’s fieldwork (rainfall simulator experiments) and RUSLE model calculations (2024–2026).

Consequently, K_final_scaled provides a more reliable relative representation of soil erodibility compared to the conventional K-factor, by indirectly integrating physical properties, particularly those related to plasticity.

The rainfall simulator measurements provide qualitative field support for the model’s ability to capture relative erosion trends. Both the model predictions and field measurements consistently indicate higher erosion in flysch and cultivated areas, and lower erosion in calcareous and fallow areas.

However, a methodological limitation is the comparison between basin-scale RUSLE predictions (km^2) and plot-scale rainfall simulator measurements ($1\ m^2$). These spatial scales are fundamentally different. Therefore, we interpret this comparison as a qualitative assessment of trends rather than a quantitative validation. The agreement between the two approaches supports the overall trend captured by the developed model, but the absolute values should not be directly compared. Future studies should consider long-term monitoring at larger spatial scales.

Beyond the scale mismatch, it is important to recognize that soil erosion models, including the present K_ID approach, are inherently predictive and not designed to produce exact quantitative estimates. Their primary value lies in providing relative spatial rankings and identifying erosion-prone areas. The developed K-factor represents an improvement in this regard compared to the conventional method. Further refinement through additional field data and model integration will be needed to reduce the remaining gap between predicted and observed values.

A limitation of this study is the absence of independent external validation. The model was developed and evaluated using the same dataset ($n = 11$). Although LOOCV indicated internal consistency ($R^2 = 0.985$), this does not replace validation on an independent dataset. Future work should prioritize testing the K_ID model using independent datasets from other Mediterranean basins to confirm its transferability and predictive robustness.

While RMSE, MAE, and bias were calculated to assess model performance, a more comprehensive uncertainty analysis (e.g., Monte Carlo simulation, Bayesian inference) was beyond the scope of this study due to the limited sample size. Future research should incorporate more advanced uncertainty quantification methods to better characterize the predictive limits of the K_ID model.

The regression model satisfied the basic statistical assumptions, as confirmed by residual diagnostics. The normality of residuals was verified using the Shapiro–Wilk test ($p = 0.12$), while homoscedasticity was assessed through visual inspection of the residuals versus fitted values plot, which showed no systematic pattern.

A more comprehensive uncertainty analysis (e.g., Monte Carlo simulation or Bayesian inference) and advanced statistical modeling (e.g., mixed-effects models) were beyond the scope of this study due to the limited sample size ($n = 11$). Future research should incorporate more advanced uncertainty quantification methods to better characterize the predictive limits of the K_ID model.

Nevertheless, the reported performance metrics (RMSE, MAE, bias, and confidence intervals) provide a consistent and reliable basis for evaluating model performance within the constraints of the available dataset. In addition, the sensitivity analysis indicates that the model is stable and not highly dependent on the exact value of the correction factor.

Comparison of results with regional studies in the Mediterranean basin

The developed K-factor values (K_final_scaled ranging from 0.0332 to 0.2662) fall within the range reported in the literature for Mediterranean environments (Table 9).

What also distinguishes this study is that it is one of the few in northern Morocco to have conducted field validation using a rainfall simulator designed and manufactured locally according to the methodology of (Roose, 1996), Most previous studies (El Assaoui et al., 2023; Moussebbih et al., 2019) relied solely on modeling without independent field validation. This significantly enhances the credibility of the developed $K_{\_final\_scaled}$ factor.

Practical implications for soil management in northern Morocco

Instead of relying on (Wischmeier and Smith, 1978) equations based solely on particle size distribution and organic matter, it is recommended to integrate the plasticity index (PI) and the lithological factor when mapping soil erodibility. This approach is economically simpler (Atterberg limits are less costly than detailed particle size analysis).

Since erosion is concentrated in specific hotspots (due to variability in lithology, slope, and land use), management efforts should be directed toward these hotspots rather than being uniformly distributed across the entire basin.

Sample S2 demonstrated that soil with dense vegetation cover (88.89%) and high organic matter content (5.24%) can resist erosion effectively despite high clay content. Therefore, conservation tillage, soil cover, and organic matter addition should be encouraged.

The developed equation (K_ID = 0.0913 × ln (PI) – 0.0385) with the lithological factor can be tested in other Mediterranean regions with similar geological characteristics (northern Algeria, Tunisia, southern Spain, Italy, Greece) to enhance the model's generalizability.

Study limitations

The sample size is limited (n = 11), although the samples represent the main lithological units covering most of the basin area (~85%). A larger dataset would improve model robustness and statistical reliability.

No external validation dataset was available. Although LOOCV ($R^2 = 0.985$) confirms internal consistency, it does not replace independent validation across other Mediterranean basins.

The model is locally calibrated, and the correction factor (0.603587229) is an empirical parameter specific to the Oued Aoudour basin and requires recalibration before application elsewhere.

A scale mismatch exists between basin-scale RUSLE outputs and plot-scale rainfall simulator measurements. Therefore, the comparison is interpreted as a qualitative trend assessment rather than a strict quantitative validation.

CONCLUSIONS

This study developed a locally calibrated soil erodibility factor for the Oued Aoudour basin based on the PI and lithological controls, with qualitative field support from a custom-built rainfall simulator. The model was designed to provide improved relative estimates of soil erosion rather than absolute quantitative predictions, acknowledging the inherent uncertainties in erosion modeling.

The logarithmic relationship between PI and K improved the coefficient of determination from $R^2 = 0.465$ to $R^2 = 0.9918$ after integrating a lithological factor and an empirical correction factor (0.603587229). The developed K-factor ranged from 0.0332 (calcareous soils) to 0.2662 (flysch soils), with estimated soil loss averaging 39 t/ha/year — a 32% improvement over the conventional K-factor (52 t/ha/year). Leave-one-out cross-validation ($R^2 = 0.985$) confirmed internal stability, though external validation using independent datasets remains necessary.

Spatial analysis showed that erosion is concentrated in hotspots occupying 13.5% of the basin, with Jenks thresholds at 9.3, 24, and 47 t/ha/year. Site-level comparisons confirmed that surface condition and land use can override textural controls on erosion.

Table 9. Comparison of K-factor ranges in Mediterranean environments

Region	Source	K-factor range
Southern Spain	(Martínez-Murillo et al., 2013)	0.07–0.21
Northern Italy	(Panagos et al., 2018)	Up to 0.30
Northern Morocco (Rif)	(Sadiki et al., 2004)	0.02–0.35
Oued Aoudour basin (this study)	K_final_scaled	0.0332–0.2662

The study acknowledges several limitations, including limited sample size (n=11), absence of independent external validation, local calibration of the correction factor, and scale mismatch between plot-scale rainfall simulator experiments and basin-scale RUSLE predictions. Future research should prioritize external validation using independent datasets, long-term monitoring at larger spatial scales, and integration with other physically based models.

Practically, the study recommends targeting conservation efforts toward erosion hotspots, integrating PI and lithological factors in K-factor mapping, and promoting vegetation cover and organic matter addition. The developed K_ID model represents a step forward in improving relative estimates of soil erodibility in Mediterranean environments, with potential applicability to other basins subject to local recalibration.

Acknowledgements

The authors thank the staff of the National School of Agriculture of Meknes (ENA Meknès) for laboratory support and the local farmers of the Oued Aoudour basin for facilitating field access during soil sampling and rainfall simulation experiments. The authors also acknowledge the methodological contribution of (Roose, 1996) in the development of rainfall simulation approaches used in this study.

REFERENCES

1. Acharki, S., El Qorchi, F., Arjdal, Y., Amharref, M., Bernoussi, A.S., Ben Aissa, H., (2022). Soil erosion assessment in Northwestern Morocco. *Remote Sensing Applications: Society and Environment 25*, 100663. https://doi.org/10.1016/j.rsase.2021.100663
2. Administration des Eaux et Forêts et de la Conservation des Sols, (1995). *Plan d'aménagement anti-érosif du bassin versant de l'Oued Ouergha en amont du barrage Al Wahda : 1ère phase, analyse de la situation actuelle (Rapport principal).* Ministère de l'Agriculture et de la Mise en Valeur Agricole, Royaume du Maroc, Rabat, Maroc.
3. Afenzar, M., Abahrour, M., El Bakkari, M., Achiban, H., (2026). Évaluation de l'érosion hydrique dans le bassin versant d'Oued Aghrouz (Maroc): approche comparative entre la modélisation RUSLE et la simulation de pluie. *Revista de Estudios Andaluces (REA)* 88–114. https://doi.org/https://doi.org/10.12795/rea.2026.i51.10
4. Agence du Bassin Hydraulique du Sebou, (2026). *Données climatiques (précipitations/température) pour les stations de Tabouda, Tafrante, Bab Taza et Malha, 1989–2026* [Jeu de données non publié]. Agence du Bassin Hydraulique du Sebou, Fès, Morocco.
5. Amhani, Z., Tribak, A., (2022). *Cartographie de l'utilisation des sols et de l'érosion hydrique dans le bassin versant de l'Oued Lahdar (Prérif oriental-Maroc): Utilisation des données de la télédétection et du modèle RUSLE.* https://doi.org/10.13137/2282-572X/33429
6. Aoufa, M., Baghdad, B., El Hadi, H., Chakiri, S., Hamoud, A., Zoraa, N., Zerdeb, M.A., Moussa, K., (2022). Quantification and Evaluation of Water Erosion by RUSLE/GIS Approach in the Ykem Watershed (Western Morocco). *Ecol. Eng. Environ. Technol. 23*, 42–53. https://doi.org/10.12912/27197050/151631
7. Brahim, B., Meshram, S.G., Abdallah, D., Larbi, B., Drisss, S., Khalid, M., Khedher, K.M., (2020). Mapping of soil sensitivity to water erosion by RUSLE model: case of the Inaouene watershed (Northeast Morocco). *Arab J Geosci 13*, 1153. https://doi.org/10.1007/s12517-020-06079-y
8. Dahman, L., Merzouk, A., Sabir, M., Fenjiro, I., (1997). Cartographie des pertes en terre dues à l'érosion hydrique par utilisation d'un système d'information géographique et des images satellitaires. Cas du bassin versant de Telata, in: *Atelier de Travail Sur La Modélisation de l'érosion Hydrique Par «RUSLE»*. pp. 52–65.
9. Domfeh, M.K., Boakye, E.K., Ankrah, J.K., Kuunifaa, C.B., Sey, N.E.N., Nyantakyi, E.K., Amproche, A.A., Wusah, R.B., (2026). Soil erosion assessment in the White Volta River Basin using USLE and RUSLE models: implications on the Pwalugu Multipurpose Dam Project. *CATENA 268*, 110043. https://doi.org/10.1016/j.catena.2026.110043
10. Duarte, L., Teodoro, A.C., 2021. GIS open-source plugins development: A 10-year bibliometric analysis on scientific literature. *Geomatics 1*, 206–245. https://doi.org/10.3390/geomatics1020013
11. Ed-Dakiri, S., Etebaai, I., Moussaoui, S.E., Tawfik, A., Lamgharbaj, M., Talibi, H.E., Dekkaki, H.C., Taher, M., (2024). Assessing soil erosion risk through geospatial analysis and magnetic susceptibility: A study in the Oued Ghiss dam watershed, Central Rif, Morocco. *Scientific African 26*, e02401. https://doi.org/10.1016/j.sciaf.2024.e02401
12. El Assaoui, N., Bouiss, C., Sadok, A., (2023). Assessment of water erosion by integrating RUSLE model, GIS and remote sensing – Case of Tamdrost Watershed (Morocco). *Ecol. Eng. Environ. Technol. 24*, 43–53. https://doi.org/10.12912/27197050/159530
13. El-Ommal, M., Tribak, A., (2023). Hydrodynamic

and erosive behavior of vertisols in the Wadi Sra catchment (Central Rif, Morocco) – Analysis of the rainfall simulation results. *J. Ecol. Eng. 24*, 66–77. https://doi.org/10.12911/22998993/161202

14. Ezzahraa Bouayad, F., El Idrysy, M., Ouallali, A., El Amrani, M., Courba, S., Hahou, Y., Karim Benhachmi, M., Spalevic, V., Briak, H., (2023). Assessing soil erosion dynamics in the Rmel Watershed, Northern Morocco by using the RUSLE model, GIS, and remote sensing integration. *AgricultForest 69*. https://doi.org/10.17707/AgricultForest.69.4.11
15. FAO, (2015). *Status of the World's Soil Resources: Main Report*. FAO.
16. Ghadouani, I., Machouri, N., (2026). *L'érosion hydrique entre modélisation et diagnostic spatial.* Espaces No 15_Ar-Fr, modélisation et développement durable. https://doi.org/10.34874/PRSM/ESPACES-7659
17. Issaka, S., Ashraf, M.A., (2017). Impact of soil erosion and degradation on water quality: A review. *Geology, Ecology, and Landscapes 1*, 1–11. https://doi.org/10.1080/24749508.2017.1301053
18. Khan, K.A., Mahmood, S.A., Haseeb, M., (2026). From climatic moderation to persistent hotspots: decadal insights into soil erosion risk from RUSLE–GIS modeling in the northwestern mountains of Pakistan. *CATENA 269*, 110120. https://doi.org/10.1016/j.catena.2026.110120
19. Laouina, A., (2010). Conservation des eaux et des sols au Maroc : prise en compte de la diversité géographique. *Norois 214*, 85–99. https://doi.org/10.4000/norois.3156
20. Manaouch, M., Zouagui, A., Fenjiro, I., (2021). A review of soil erosion modeling by R/USLE in Morocco: Achievements and limits. *E3S Web Conf. 234*, 00067. https://doi.org/10.1051/e3sconf/202123400067
21. Martínez-Murillo, J.F., Nadal-Romero, E., Regüés, D., Cerdà, A., Poesen, J., (2013). Soil erosion and hydrology of the western Mediterranean badlands throughout rainfall simulation experiments: A review. *CATENA 106*, 101–112. https://doi.org/10.1016/j.catena.2012.06.001
22. Moussebbih, A., Souissi, M., Larabi, A., (2019). Modeling and mapping of the water erosion risk using GIS/RUSLE approach in the Bouregreg river watershed. *International Journal of Mechanical and Production Engineering 9*, 1605–1618.
23. Najem, H., Sadkaoui, D., Mihraje, A., Benzougagh, B., Akazzim, M., Ouadjane, Y., Khedher, K.M., Almazroui, M., Santos, C.A.G., Jaufer, L., Kader, S., (2026). A novel approach for quantifying and spatializing soil water erosion in semi-arid ecosystems using RUSLE and geospatial tools. *Physics and Chemistry of the Earth, Parts A/B/C 144*, 104464. https://doi.org/10.1016/j.pce.2026.104464
24. Nzereogu, S.K., Igwe, O., Emeh, C.O., Ukor, K.P., Echezona, P.E., (2023). Comparative analysis of the expansion rate and soil erodibility factor of some gullies in Nnewi and Nnobi, Southeastern Nigeria. *Sci Rep 13*, 15293. https://doi.org/10.1038/s41598-023-42320-w
25. Panagos, P., Standardi, G., Borrelli, P., Lugato, E., Montanarella, L., Bosello, F., (2018). Cost of agricultural productivity loss due to soil erosion in the European Union: From direct cost evaluation approaches to the use of macroeconomic models. *Land Degrad Dev 29*, 471–484. https://doi.org/10.1002/ldr.2879
26. Rehman, M.A., Abd Rahman, N., Rosli, R.N., Jusoh, M.N.H., Sharil, S., Mohd Razali, S.F., (2025). Relationship between plasticity index and soil erodibility: a case study of central Malaysian tropical soils. *Sci Rep 15*, 40748. https://doi.org/10.1038/s41598-025-24597-1
27. Renard et al, K., G, G, D, (1997). *Predicting soil erosion by water: a guide to conservation planning with the Revised Universal Soil Loss Equation (RUSLE).* Washington, D.C.
28. Roose, E., (1996). *Méthodes de mesure des états de surface du sol, de la rugosité et des autres caractéristiques qui peuvent aider au diagnostic de terrain des risques de ruissellement et d'érosion, en particulier sur les versants des montagnes,* in: De Noni, G., Lamachère, J.-M., Roose, E. (Eds.), Etats de Surface Du Sol et Risques de Ruissellement et d'érosion, Bulletin - Réseau Erosion. Paris, France, pp. 87–97.
29. Roose, E., Godefroy, J., (1968). Lessivage des éléments fertilisants en bananeraie. Fruits 23, 580–584.
30. Sadiki, A., Bouhlassa, S., Auajjar, J., Faleh, A., Macaire, J.-J., 2004. Utilisation d'un SIG pour l'évaluation et la cartographie des risques d'érosion par l'Equation universelle des pertes en sol dans le Rif oriental (Maroc) : cas du bassin versant de l'oued Boussouab. *Bulletin de l'Institut Scientifique, Rabat, Section Sciences de la Terre* 69–79.
31. Sonderegger, T., Pfister, S., (2021). Global assessment of agricultural productivity losses from soil compaction and water erosion. *Environ. Sci. Technol. 55*, 12162–12171. https://doi.org/10.1021/acs.est.1c03774
32. Wischmeier, W.H., Smith, D.D., (1978). *Predicting rainfall erosion losses - A Guide to conservation Planning.,* Département of Agriculture. U.S.A.